Environmentally Sensitive Silver Nanoparticles of Controlled Size Synthesized with PNIPAM as a Nucleating and Capping Agent

J. Ruben Morones[†,‡] and Wolfgang Frey*[,‡,§]

Departments of Chemical and Biomedical Engineering and Center for Nano and Molecular Science and Technology, The University of Texas at Austin, 1 University Station, C0800, Austin, Texas 78712

Received March 22, 2007. In Final Form: May 15, 2007

Metal nanoparticles combined with environmentally sensitive polymers can lead to enhanced nanometer-sized switches. We present a silver nanoparticle synthesis method that uses poly(*N*-isopropylacrylamide) (PNIPAM) as the nucleating, capping, and stabilizing agent. The synthesis is performed at room temperature by sodium borohydride-mediated reduction of silver nitrate in the presence of a fully hydrated polymer. The resulting metal nanoparticles have a narrow size distribution comparable to or better than those achieved with other synthesis methods. The silver particles can be thermally precipitated by the collapse of the PNIPAM shell and resolubilized with fast response times, as shown by surface plasmon spectroscopy. The silver−PNIPAM composite allows for combined surface plasmon and thermal switching applications.

Introduction

The development of nanometer-sized tools and materials that can perform a desired action upon a local or external stimulus is one major goal of bionanotechnology.[1−5] One important class of tools is environmentally sensitive polymers capable of recognizing or responding to external physical stimuli such as light, either directly[6−12] or indirectly,[13,14] and heat[12,15−22] or chemical stimuli, such as pH[16,23] and chemical ligands.[12] Such environmentally sensitive polymers, if combined with metal nanoparticles, create amplified light sensitive and locally controlled actuators that have applications as drug delivery vehicles,[24,25] microfluidic devices,[26,27] and in therapeutic ablation.[28,29]

Polymer−metal nanoparticle (P−MNP) composites are fabricated either by simple entrapment of gold or silver MNPs in a polymer gel,[13,24,25,27] by immobilization of an initiator on the MNP surface followed by surface-initiated living radical polymerization based on reversible addition−fragmentation chain reactions (RAFT),[30−32] by thiol-supported adsorption of a polymer,[33] or by in situ formation of the MNPs during polymerization.[34−37] Physical entrapment of MNPs, however,

* Corresponding author. E-mail: wfrey@mail.utexas.edu.
† Department of Chemical Engineering.
‡ Center for Nano and Molecular Science and Technology.
§ Department of Biomedical Engineering.

(1) Whitesides, G. M. The "right" size in nanobiotechnology. *Nat. Biotechnol.* **2003**, *21* (10), 1161−1165.
(2) Langer, R.; Tirrell, D. A. Designing materials for biology and medicine. *Nature* **2004**, *428* (6982), 487−492.
(3) Lahann, J.; Langer, R. Smart materials with dynamically controllable surfaces. *MRS Bull.* **2005**, *30* (3), 185−188.
(4) Peppas, N. A.; Hilt, J. Z.; Khademhosseini, A.; Langer, R. Hydrogels in biology and medicine: From molecular principles to bionanotechnology. *Adv. Mater.* **2006**, *18* (11), 1345−1360.
(5) Mavroidis, C.; Dubey, A.; Yarmush, M. L. Molecular machines. *Annu. Rev. Biomed. Eng.* **2004**, *6*, 363−395.
(6) Irie, M.; Kungwatchakun, D. Stimuli-responsive polymers−Photostimulated reversible phase separation of aqueous solutions of poly(*N*-isopropylacrylamide) with pendant azobenzene groups. *Proc. Jpn. Acad., Ser. B* **1992**, *68* (8), 127−132.
(7) Shimoboji, T.; Larenas, E.; Fowler, T.; Kulkarni, S.; Hoffman, A. S.; Stayton, P. S. Photoresponsive polymer−enzyme switches. *Proc. Natl. Acad. Sci. U.S.A.* **2002**, *99* (26), 16592−16596.
(8) Shimoboji, T.; Larenas, E.; Fowler, T.; Hoffman, A. S.; Stayton, P. S. Temperature-induced switching of enzyme activity with smart polymer−enzyme conjugates. *Bioconjugate Chem.* **2003**, *14* (3), 517−525.
(9) Akiyama, H.; Tamaoki, N. Polymers derived from *N*-isopropylacrylamide and azobenzene-containing acrylamides: Photoresponsive affinity to water. *J. Polym. Sci., Part A: Polym. Chem.* **2004**, *42* (20), 5200−5214.
(10) Natansohn, A.; Rochon, P. Photoinduced motions in azo-containing polymers. *Chem. Rev.* **2002**, *102* (11), 4139−4175.
(11) Kamenjicki, M.; Lednev, I. K.; Asher, S. A. Photoresponsive azobenzene photonic crystals. *J. Phys. Chem. B* **2004**, *108* (34), 12637−12639.
(12) Qiu, Y.; Park, K. Environmentally sensitive hydrogels for drug delivery. *Adv. Drug Deliv. Rev.* **2001**, *53* (3), 321−339.
(13) Sershen, S. R.; Westcott, S. L.; West, J. L.; Halas, N. J. An opto-mechanical nanoshell−polymer composite. *Appl. Phys. B* **2001**, *73* (4), 379−381.
(14) Hirsch, L. R.; Gobin, A. M.; Lowery, A. R.; Tam, F.; Drezek, R. A.; Halas, N. J.; West, J. L. Metal nanoshells. *Ann. Biomed. Eng.* **2006**, *34* (1), 15−22.
(15) Schild, H. G. Poly(*N*-isopropylacrylamide)−Experiment, theory, and application. *Progr. Polym. Sci.* **1992**, *17* (2), 163−249.
(16) Gil, E. S.; Hudson, S. A. Stimuli-reponsive polymers and their bioconjugates. *Progr. Polym. Sci.* **2004**, *29* (12), 1173−1222.
(17) Stayton, P. S.; Shimoboji, T.; Long, C.; Chilkoti, A.; Chen, G. H.; Harris, J. M.; Hoffman, A. S. Control of protein−ligand recognition using a stimuli-responsive polymer. *Nature* **1995**, *378* (6556), 472−474.
(18) Meyer, D. E.; Chilkoti, A. Purification of recombinant proteins by fusion with thermally responsive polypeptides. *Nat. Biotechnol.* **1999**, *17* (11), 1112−1115.
(19) Meyer, D. E.; Chilkoti, A. Quantification of the effects of chain length and concentration on the thermal behavior of elastin-like polypeptides. *Biomacromolecules* **2004**, *5* (3), 846−851.
(20) Frey, W.; Meyer, D. E.; Chilkoti, A. Dynamic addressing of a surface pattern by a stimuli-responsive fusion protein. *Adv. Mater.* **2003**, *15* (3), 248−251.
(21) Frey, W.; Meyer, D. E.; Chilkoti, A. Thermodynamically reversible addressing of a stimuli responsive fusion protein onto a patterned surface template. *Langmuir* **2003**, *19* (5), 1641−1653.
(22) Yang, J.; Yamato, M.; Okano, T. Cell-sheet engineering using intelligent surfaces. *MRS Bull.* **2005**, *30* (3), 189−193.
(23) Peppas, N. A.; Kim, B. Stimuli-sensitive protein delivery systems. *J. Drug Deliv. Sci. Technol.* **2006**, *16* (1), 11−18.
(24) Sershen, S. R.; Westcott, S. L.; Halas, N. J.; West, J. L. Temperature-sensitive polymer−nanoshell composites for photothermally modulated drug delivery. *J. Biomed. Mater. Res.* **2000**, *51* (3), 293−298.
(25) Skirtach, A. G.; Javier, A. M.; Kreft, O.; Kohler, K.; Alberola, A. P.; Mohwald, H.; Parak, W. J.; Sukhorukov, G. B. Laser-induced release of encapsulated materials inside living cells. *Angew. Chem., Int. Ed.* **2006**, *45* (28), 4612−4617.
(26) Huber, D. L.; Manginell, R. P.; Samara, M. A.; Kim, B. I.; Bunker, B. C. Programmed adsorption and release of proteins in a microfluidic device. *Science* **2003**, *301* (5631), 352−354.
(27) Sershen, S. R.; Mensing, G. A.; Ng, M.; Halas, N. J.; Beebe, D. J.; West, J. L. Independent optical control of microfluidic valves formed from optomechanically responsive nanocomposite hydrogels. *Adv. Mater.* **2005**, *17* (11), 1366−1368.
(28) Hirsch, L. R.; Stafford, R. J.; Bankson, J. A.; Sershen, S. R.; Rivera, B.; Price, R. E.; Hazle, J. D.; Halas, N. J.; West, J. L. Nanoshell-mediated near-infrared thermal therapy of tumors under magnetic resonance guidance. *Proc. Natl. Acad. Sci. U.S.A.* **2003**, *100* (23), 13549−13554.
(29) O'Neal, D. P.; Hirsch, L. R.; Halas, N. J.; Payne, J. D.; West, J. L. Photothermal tumor ablation in mice using near infrared-absorbing nanoparticles. *Cancer Lett.* **2004**, *209* (2), 171−176.

10.1021/la7008336 CCC: $37.00
Published on Web 06/23/2007

often produces heterogeneous composites, and MNP synthesis during the polymerization provides less control over the MNP size dispersity.

The most commonly used temperature-sensitive polymer is poly(*N*-isopropylacrylamide) (PNIPAM), which has a lower critical solution temperature (LCST) of 32 °C.[15] The intrinsically temperature -sensitive PNIPAM can be made light sensitive based on the resonance absorption of MNPs in the visible or near-infrared wavelength range, exploiting the localized surface plasmon resonance (LSPR) in small gold and silver nanoparticles and the conversion of the absorbed energy into heat. The optical properties of these metal nanoparticles depend very strongly on their size and shape, the refractive index of the surrounding medium, and the distance between neighboring particles.[38]

Gold and silver nanoparticle synthesis is most often performed by wet chemistry: a metal salt precursor is reduced to its metallic form by a reducing agent such as ethylene glycol,[39] sodium citrate,[40] or sodium borohydride.[41] Growth, size, and colloidal stability are controlled by using a stabilizing or capping agent.[41,42] The most common wet synthesis route for colloidal silver particles is the reduction of $AgNO_3$ in the presence of poly(vinylpyrrolidone) (PVP),[39,42] which achieves stable nanostructures with controlled shapes[43] and sizes.[42] However, in the production of nanocomposites, coupling with a responsive polymer requires the PVP to be removed, followed by a selective grafting process, typically with thiols.

Although MNP growth and colloidal stability are most often controlled by PVP, other polymers, such as acrylamide[34,36,37] or acrylonitrile,[35] have been used as well. Several one-pot synthesis approaches have used γ-irradiation,[36,37] UV-irradiation,[44] high temperature,[34] or a chemical initiator[35,45] simultaneously for the polymerization and as the reducing agent, while the growing polymer also acts as the capping agent. Similarly, a simultaneous reduction of silver and copolymerization of NIPAM or oligo-NIPAM with styrene has been demonstrated using azobis-isobutyronitril (AIBN) as the reducing agent with a dehydrated PNIPAM above the LCST. However, the use of a chemical initiator as the reducing agent leads to a broadening of the particle size distribution.[46,47]

Here, we report on a two-step procedure in which we first produce PNIPAM of a defined molecular weight and then use the polymer to nucleate and control the reduction of silver and stabilize the resulting environmentally sensitive nanocomposite by embedding the silver nanoparticles in a cocoon of PNIPAM. Reduction of silver is performed with sodium borohydride at room temperature, which allows for the polymer to stay in solution until the reduction is completed or stopped. The particles undergo a reversible precipitation upon external stimulus by temperature, which leads to a small shift of the LSPR peak in the extinction spectrum, indicating that the particles keep their polymer shell and do not aggregate closely. The kinetics of the thermally driven phase transition is fast in both directions, indicating a low interpenetration of the polymers.

Experimental Procedures

Materials. Deionized water with a resistivity of at least 18.0 MΩ cm (EPure, Barnstead Thermolyne) was used in all experiments. NIPAM (Fisher Scientific) was recrystallized once in hexane (Fisher Scientific) and stored at −20 °C until use. Sodium borohydride (Fisher Scientific), silver nitrate, *N*,*N*,*N*′,*N*′-tetramethylethylene diamine (TEMED), and ammonium persulfate (APS) (all Sigma Aldrich) were used as purchased.

Polymer Synthesis. PNIPAM was obtained by free radical polymerization of NIPAM using an APS and TEMED redox initiator system. Nitrogen was bubbled through 200 mL of a 0.3 M aqueous NIPAM solution for 20 min and then sealed under a nitrogen atmosphere during reaction. The polymerization was started by the addition of 1% (wt) of each of the redox system components and left to proceed for 2 h. The PNIPAM product was poured into 4 times the volume of ethanol for precipitation, followed by centrifugation at 16 600*g* for 15 min, then resuspension in water. This procedure was repeated 3 times to remove any unreacted monomer or initiator from the solution. The aqueous polymer solution was freeze dried and stored at −20 °C in powder form until further use. Gel permeation chromatography (GPC) determined the mass average molecular weight of the polymer used in these experiments to be $M_w = 396\,000$ with a polydispersity index of 1.54. GPC experiments were performed using tetrahydrofuran (THF) as an eluent in a Waters 515 HPLC solvent pump and two PLgel mixed-C columns (5 μm bead size for M_w range of 200−2 000 000 g/mol) (Polymer Laboratories, Inc.).

Preparation of Ag−PNIPAM Colloids. Aqueous mixtures of 1 mM silver nitrate and PNIPAM at indicated molar ratios of PNIPAM/Ag were prepared and stirred at room temperature. After 5 min of stirring, $NaBH_4$ was added to achieve a 3:1 molar ratio of $NaBH_4/Ag^+$. The solution was stirred for 5 min to react and then immediately diluted with water to 4 times the volume to stop the reaction. The diluted solution was then heated to 40 °C during centrifugation at 16 600*g* for 15 min to sequentially precipitate Ag−PNIPAM and then the polymer. The Ag−PNIPAM nanoparticles

(30) Raula, J.; Shan, J.; Nuopponen, M.; Niskanen, A.; Jiang, H.; Kauppinen, E. I.; Tenhu, H. Synthesis of gold nanoparticles grafted with a thermoresponsive polymer by surface-induced reversible addition−fragmentation chain-transfer polymerization. *Langmuir* **2003**, *19* (8), 3499−3504.

(31) Zhu, M. Q.; Wang, L. Q.; Exarhos, G. J.; Li, A. D. Q. Thermosensitive gold nanoparticles. *J. Am. Chem. Soc.* **2004**, *126* (9), 2656−2657.

(32) Shan, J.; Nuopponen, M.; Jiang, H.; Viitala, T.; Kauppinen, E.; Kontturi, K.; Tenhu, H. Amphiphilic gold nanoparticles grafted with poly(*N*-isopropylacrylamide) and polystyrene. *Macromolecules* **2005**, *38* (7), 2918−2926.

(33) Nath, N.; Chilkoti, A. Interfacial phase transition of an environmentally responsive elastin biopolymer adsorbed on functionalized gold nanoparticles studied by colloidal surface plasmon resonance. *J. Am. Chem. Soc.* **2001**, *123* (34), 8197−8202.

(34) Chen, M.; Wang, L. Y.; Han, J. T.; Zhang, J. Y.; Li, Z. Y.; Qian, D. J. Preparation and study of polyacryamide-stabilized silver nanoparticles through a one-pot process. *J. Phys. Chem. B* **2006**, *110* (23), 11224−11231.

(35) Zhang, Z. P.; Han, M. Y. One-step preparation of size-selected and well-dispersed silver nanocrystals in polyacrylonitrile by simultaneous reduction and polymerization. *J. Mater. Chem.* **2003**, *13* (4), 641−643.

(36) Zhu, Y. J.; Qian, Y. T.; Li, X. J.; Zhang, M. W. γ-Radiation synthesis and characterization of polyacrylamide−silver nanocomposites. *Chem. Commun.* **1997**, *12*, 1081−1082.

(37) Zhu, Y. J.; Qian, Y. T.; Li, X. J.; Zhang, M. W. A non-aqueous solution route to synthesis of polyacrylamide−silver nanocomposites at room temperature. *Nanostruct. Mater.* **1998**, *10* (4), 673−678.

(38) Hutter, E.; Fendler, J. H. Exploitation of localized surface plasmon resonance. *Adv. Mater.* **2004**, *16* (19), 1685−1706.

(39) Silvert, P. Y.; Herrera-Urbina, R.; Duvauchelle, N.; Vijayakrishnan, V.; Elhsissen, K. T. Preparation of colloidal silver dispersions by the polyol process. 1. Synthesis and characterization. *J. Mater. Chem.* **1996**, *6* (4), 573−577.

(40) Henglein, A.; Giersig, M. Formation of colloidal silver nanoparticles: Capping action of citrate. *J. Phys. Chem. B* **1999**, *103* (44), 9533−9539.

(41) Van Hyning, D. L.; Zukoski, C. F. Formation mechanisms and aggregation behavior of borohydride reduced silver particles. *Langmuir* **1998**, *14* (24), 7034−7046.

(42) Silvert, P. Y.; Herrera-Urbina, R.; Tekaia Elhsissen, K. Preparation of colloidal silver dispersions by the polyol process. 2. Mechanism of particle formation. *J. Mater. Chem.* **1997**, *7* (2), 293−299.

(43) Wiley, B.; Sun, Y. G.; Chen, J. Y.; Cang, H.; Li, Z. Y.; Li, X. D.; Xia, Y. N. Shape-controlled synthesis of silver and gold nanostructures. *MRS Bull.* **2005**, *30* (5), 356−361.

(44) Zhou, Y.; Wang, C. Y.; Zhu, Y. R.; Chen, Z. Y. A novel ultraviolet irradiation technique for shape-controlled synthesis of gold nanoparticles at room temperature. *Chem. Mater.* **1999**, *11* (9), 2310−2312.

(45) Zhou, Y.; Hao, L. Y.; Zhu, Y. R.; Hu, Y.; Chen, Z. Y. A novel ultraviolet irradiation technique for fabrication of polyacrylamide−metal (M = Au, Pd) nanocomposites at room temperature. *J. Nanoparticle Res.* **2001**, *3* (5−6), 379−383.

(46) Chen, C. W.; Chen, M. Q.; Serizawa, T.; Akashi, M. In situ formation of silver nanoparticles on poly(*N*-isopropylacrylamide)-coated polystyrene microspheres. *Adv. Mater.* **1998**, *10* (14), 1122−1126.

(47) Chen, C. W.; Serizawa, T.; Akashi, M. Synthesis and characterization of poly(*N*-isopropylacrylamide)-coated polystyrene microspheres with silver nanoparticles on their surfaces. *Langmuir* **1999**, *15* (23), 7998−8006.

were recovered by centrifugation at 25 700*g* for 10 min and then resuspended in water. This process was performed twice, followed by freeze drying to recuperate the nanocomposite in a powder form for storage at −20 °C.

Transmission Electron Microscopy (TEM). TEM images were obtained with a JEOL 2010-F at an acceleration voltage of 400 kV. The specimens were prepared by placing a drop of aqueous colloidal suspension onto a carbon-coated copper grid, incubating for 30 min, and then aspirating the excess solvent with filter paper. Shape and size distributions were determined from enlarged photographs of the TEM images using at least 400 particles for each sample. Diffraction patterns from individual silver nanoparticles were collected in TEM diffraction mode at an acceleration voltage of 200 kV. Negatives were scanned at 3200 dpi for crystal diffraction analysis. For negative staining, a solution of 0.1% w/v uranyl acetate in water was placed on a piece of Parafilm, and a TEM grid, prepared as described previously, was placed on top of the drop for 1 min. Afterward, the sample was dried using a filter paper and left to dry overnight. The sample was then analyzed by TEM as described previously.

UV−vis Spectroscopy. The LCST of PNIPAM alone and the spectral properties of PNIPAM−Ag colloids in aqueous solution were measured on a temperature-controlled CARY 5000 UV−vis spectrophotometer. When needed, the temperature was raised from 25 to 36 °C at a rate of 1 °C/min. Recorded spectra were analyzed for peak position, peak width, and area under the peak of the LSPR resonance. To separate the LSPR signal from spectra of cloudy suspensions, the spectra were fitted with a function $f(\lambda) = 1/\lambda^x$ (λ = wavelength and $x \approx 4$ as expected for Rayleigh−Gans scattering[48]). The fitting eliminates the scattering component of the sample, which is caused by the agglomeration of the colloid, which is in turn driven by the phase transition of PNIPAM. The fit excluded the wavelength range of 350−650 nm to avoid fit distortions from the plasmon peak. Once the scattering was subtracted, the remaining curve was fitted with a polynomial around the maximum to determine the position of the plasmon peak.

Modeling of the Absorption Spectra. Mie theory for spherical particles and spherical concentric core shell particles was used to model the experimental extinction spectra. The model for individual particles was adapted from code in ref 49 and written in IGOR Pro (Wavemetrics). The standard code was extended to include convoluted spectra assuming a Gaussian distribution of particle sizes, using the measured mean and standard deviation. The bulk refractive index for silver was taken from ref 50 as tabulated at ref 51. To take the small particle size and associated damping into account, the Ag particle refractive index was approximated by adding a term to the imaginary part of the refractive index as described by Kreibig:[52] $\Delta\epsilon'' = (\omega_p^2 v_F \eta)/(\omega^3 R)$, where ϵ'' is the imaginary part of the refractive index of silver, ω is the frequency of the light, $\omega_p = 1.38 \times 10^{16}$ s^{-1} is the plasma frequency of silver, $v_F = 1.4 \times 10^6$ m s^{-1} is the Fermi velocity for silver, R is the silver particle radius, and $\eta \leq 1$ is a weight factor commonly set to $\eta = 1$.

Results

Synthesis and Characterization of Colloidal PNIPAM−Silver Nanoparticles. The MNP synthesis reduces silver nitrate, the metallic precursor, with the strong reducing agent $NaBH_4$, using PNIPAM of a mass average molecular weight of 396 000 to control and stabilize the reduction kinetics. The molar ratio of $NaBH_4$/Ag was kept constant at 3:1 in the presence of different molar NIPAM/Ag ratios (polymer—molar concentration in monomer units—to Ag ratio, PAR) between 360:1 and 0:1. The reaction was performed in water at 25 °C, which is below the LCST of PNIPAM, to keep the polymer available in solution during the reduction process. The reduction reaction was very rapid and was completed within 5 min. After transfer to water, the colloidal particles with at least PAR 90:1 are stable for several months, and lyophilized particles can easily be resolubilized. Colloidal particles with less than PAR 45:1 show a small degree of precipitation over the course of a week, while controls with no PNIPAM already precipitate during synthesis.

Figure 1A shows the silver colloid product in the absence of PNIPAM and demonstrates the need for a capping agent to prevent particle sintering. In comparison, examples of four PARs show round nanoparticles of defined size and with crystalline silver (Figure 1B−F), showing a diffraction typical for a fcc crystal with a lattice constant of 0.409 nm as expected.[53] The average particle size for a 5 min reduction of a 1 mM solution of $AgNO_3$ is shown in Figure 1 for each of the PARs and depends on the PNIPAM concentration in a power-law dependence (Figure 1B). The particle size varies with a standard deviation of 18−20% for PARs above 20:1, which is similar to or better than the variation seen with PVP and other capping agents.[39]

PNIPAM stabilizes and encapsulates the silver particles, which can be seen in negative-stain TEM (Figure 2). The stain outlines the polymer wrapping around the nanoparticle in a cocoon-like fashion. Figure 2 shows examples of PAR 45:1 and 180:1 with a dried PNIPAM layer thickness of 6−10 nm. The polymer encapsulation at PAR 45:1 and below is sometimes incomplete and uneven, while for the higher PARs, multiple particles are grouped.

The reaction can be followed by observing the color of the colloidal dispersion. Figure 3A shows UV−vis extinction spectra for four PARs. The non-normalized extinction peaks show a gradual shift to the red with increasing PAR, indicating changes in the environment of each particle. The two higher PARs are nearly identical. The FWHM is about 80 nm for all PARs (Figure 3B) except for PAR 45:1, for which it is much lower. The FWHM is higher than seen for PVP-capped silver nanoparticles[54] and indicates either insufficient covering at low PAR or some proximity of the metal nanoparticles at high PAR.

In Figure 3A, the Mie model extinction spectra for spherical concentric shells have been overlaid for silver particle size distributions corresponding to each PAR. The PNIPAM shell refractive index and the layer thickness were fit parameters, but because the two parameters are not completely independent, a shell thickness of 15 nm was assumed for consistency except for PAR 20:1, for which the thickness was 1 nm. This thickness is less than would be expected from a random coil of the polymer. The model, with a refractive index of 1.36 for the shell as seen for PNIPAM,[55] reproduces the maximum position and the FWHM for PAR 45:1, with both values similar to those seen for PVP[54] (Figure 3B). For PAR 20:1, a refractive index of 1.36 but only 1 nm of polymer shell reproduces the maximum position, but the

(48) Sano, Y.; Nakagaki, M. Wavelength dependence of the turbidity of spheroidal particles calculated in the Stevenson−Heller approximation. *J. Phys. Chem.* **1983**, *87* (9), 1614−1618.

(49) Bohren, C. F.; Huffman, D. R. *Absorption and Scattering of Light by Small Particles*, 1st ed.; Wiley-VCH: Weinheim, Germany, 1998.

(50) Quinten, M. Optical constants of gold and silver clusters in the spectral range between 1.5 and 4.5 eV. *Z. Phys. B: Condens. Matter* **1996**, *101* (2), 211−217.

(51) http://www.lightscattering.de/MieCalc/eindex.html; accessed February 2007.

(52) Kreibig, U. Lattice defects in small metallic particles and their influence on size effects. *Z. Phys. B: Condens. Matter* **1978**, *31* (1), 39−47.

(53) Li, Y.; Kim, Y. N.; Lee, E. J.; Cai, W. P.; Cho, S. O. Synthesis of silver nanoparticles by electron irradiation of silver acetate. *Nucl. Instrum. Methods Phys. Res., Sect. B* **2006**, *251* (2), 425−428.

(54) Slistan-Grijalva, A.; Herrera-Urbina, R.; Rivas-Silva, J. F.; Avalos-Borja, M.; Castillon-Barraza, F. F.; Posada-Amarillas, A. Classical theoretical characterization of the surface plasmon absorption band for silver spherical nanoparticles suspended in water and ethylene glycol. *Phys. E* **2005**, *27* (1−2), 104−112.

(55) Harmon, M. E.; Kuckling, D.; Frank, C. W. Photocross-linkable PNIPAAm copolymers. 2. Effects of constraint on temperature and pH-responsive hydrogel layers. *Macromolecules* **2003**, *36* (1), 162−172.

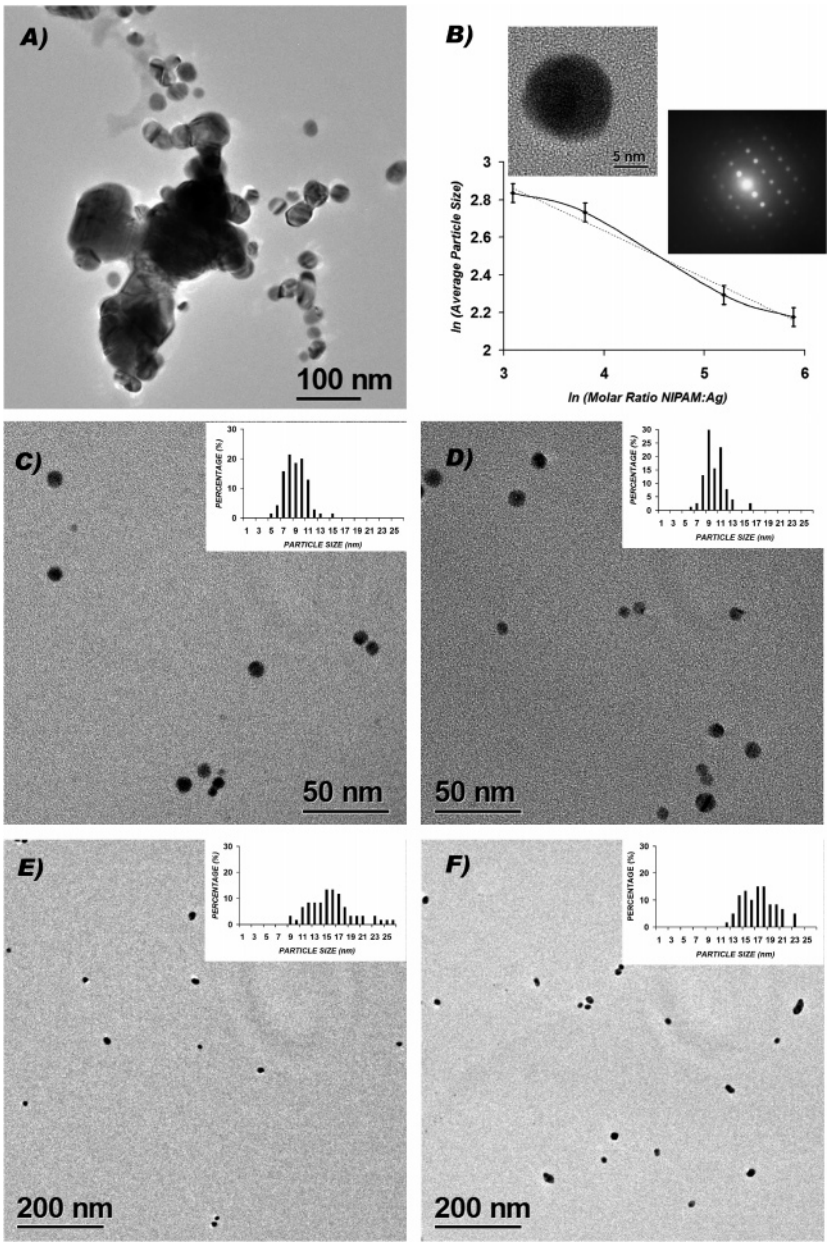

Figure 1. (A) Silver nanoparticles produced in a synthesis without PNIPAM tend to sinter. (B) Particle size as a function of the molar ratio of NIPAM monomers in PAR. A power-law relationship is found between the mean particle size and the PAR. Particles produced in the synthesis are spherical with diameters between 10 and 20 nm and are crystalline with a fcc crystal structure (inset: real-space image of a particle and electron diffraction along the [112] axis.) (C−F) Silver nanoparticles synthesized using four different PARs: the product is monodisperse and does not sinter. (C) TEM sample of PAR 360:1, (D) 180:1, (E) 90:1, and (F) 20:1. Insets in panels C−D show the size distributions of about 400 particles chosen randomly from different areas of the carbon grid.

FWHM is underestimated, and a long tail to the red is seen that indicates less size control as seen in the large tail of the size distribution in Figure 1. PARs 180:1 and 360:1 could not be fit with the literature value for the polymer refractive index, but the index had to be 1.46 to reproduce the maximum position. The measured spectra also have a larger FWHM than the model but no long tail to the red. This trend indicates that while the size control is increased with increasing PAR, there is also a tendency for more than one particle to be encapsulated in one cocoon, which can shift the maximum and broaden the plasmon peak.[56,57] Indeed, a count of particles closer than 3 nm from each other in TEM images reflects this trend: about 35−50% of the particles were in groups of two or more for PARs 360:1 and 180:1, while only 10−15% were aggregated for PAR 45:1 or 20:1. The relatively small peak shift of about 10 nm, as compared to the expected position of 405 nm, induced by the coupling of the electromagnetic fields between particles within one cocoon indicates that the metal nanoparticles do not come into direct contact.[56,57]

For four PARs and at three time points, the area under the extinction peak was determined. At a constant initial silver concentration, the area under the plasmon peak is a measure of the size and number of particles in the colloidal suspension. To test the influence of PNIPAM on the nucleation of the cluster, a very low molar ratio of $Ag/NaBH_4 = 1:0.25$ was used. The

(56) Quinten, M. Optical effects associated with aggregates of clusters. *J. Cluster Sci.* **1999**, *10* (2), 319−358.

(57) Jensen, T.; Kelly, L.; Lazarides, A.; Schatz, G. C. Electrodynamics of noble metal nanoparticles and nanoparticle clusters. *J. Cluster Sci.* **1999**, *10* (2), 295−317.

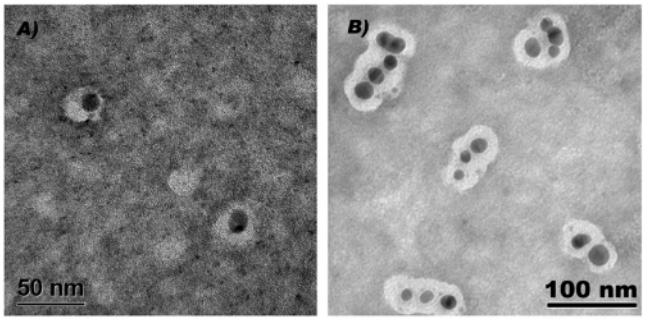

Figure 2. TEM images of Ag−PNIPAM particles negatively stained with uranyl acetate. (A) 45:1 PAR and (B) 180:1 PAR. Ag particles are entrapped in a polymer shell, either individually or in groups, and at low PAR may be uneven or incomplete.

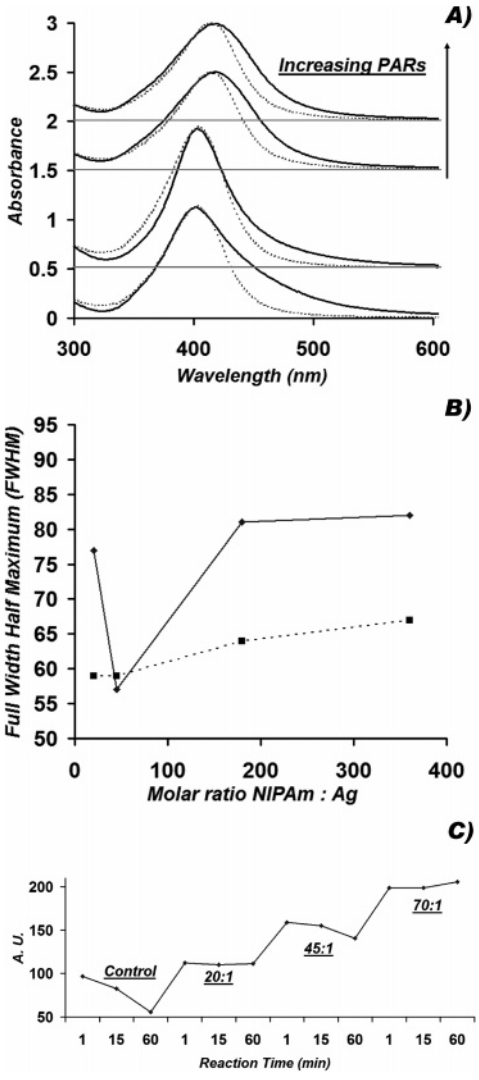

Figure 3. (A) Measured UV−vis spectra for PARs 20:1, 45:1, 180:1, and 360:1 (solid lines) and Mie core−shell model simulations (dashed lines). (B) The FWHM of the measured UV−vis peaks as a function of PAR (solid line) and theoretical values (dashed line). (C) Area under the extinction peak for four different PARs at three different times after the start of the reaction.

reaction was completed in less than a minute and was too fast to be resolved by UV−vis spectroscopy. Later time points do not lead to a change in the area under the resonance peak, except if no polymer is present, in which case it decreases with time, indicating aggregation and precipitation during the synthesis process (Figure 3C). For PARs of 20:1, 45:1, and 70:1, the area under the extinction peak increases linearly with PAR. Increasing PAR leads to a decrease in particle size (Figure 1B), which is expected to lead to a decrease in the extinction with the sixth power of the MNP radius.[49] This decrease must therefore be overcompensated by the number of particles to explain the increase in extinction with PAR. PNIPAM therefore acts not only as a capping and stabilization agent but also as a nucleation agent by increasing the number of MNPs.

Temperature Switching. The temperature dependence of the PNIPAM−Ag composite was studied using optical microscopy of concentrated, and UV−vis spectroscopy of very dilute, samples to minimize the scattering effect of the PNIPAM above the LCST. Figure 4A shows the optical transmission of a colloidal suspension switched reversibly with a fast response in both directions and no fatigue, achieved by heating and passive cooling in an optical microscope. A control experiment (not shown) with PVP-capped MNPs in the presence of PNIPAM precipitated only the PNIPAM but left the MNPs in suspension. This indicates that the precipitation of PNIPAM-capped Ag nanoparticles is induced by the conformational change of the polymer in the cocoon.

UV−vis spectra of the Ag surface plasmon resonance before and after the phase transition can give further information about the local environment of the silver particles (i.e., the state of the PNIPAM and the distance to neighboring silver particles). At temperatures above the LCST, however, scattering from the aggregated colloids dominates the spectrum (Figure 4B). To extract the surface plasmon information, a $1/\lambda^x$ background, with $x \approx 4$, was subtracted, assuming that the scattering was Rayleigh−Gans-like and that multiple scattering could be neglected.[48] Exponents were fixed at $x = 4.0$, yielding good fits and justifying these assumptions, except for PARs 180:1 and 360:1, for which the exponent was $x = 3.5$ to account for stronger scattering. Figure 4C shows a representative spectrum of the Ag−PNIPAM particles (PAR 45:1) below (25 °C) and above the LCST (36 °C) after background subtraction. The resulting spectra show a plasmon resonance that has red shifted by 12 nm (Figure 4D). Smaller shifts are seen for the other PARs. Increasing the temperature to 45 °C does not change the peak position any further.

Fits of the extinction spectra to a Mie concentric shell scattering model with a shell thickness of 6 nm, based on the TEM images (Figure 2), show a change in refractive index of about 0.08 to 0.1 units relative to the index below the LCST. The FWHM does not increase above the LCST, indicating, together with the small shift in peak position, that the silver particles see mainly a change in environment due to a more compact polymer and to a lesser degree due to an increase in proximity of the particles.[56,57]

Discussion

The growth of silver nanoparticles is controlled by the addition of polymers or surfactants, which act as nucleating and stabilization agents and control the kinetics and preferential growth direction.[42,43] For the nucleation of silver nanoparticles with PVP, the coordination of silver ions by oxygen and nitrogen is considered necessary,[42,58] and a similar coordination is assumed to take place with PNIPAM.[46,47] Our results show that PNIPAM can act as a nucleating agent, with an increased number of silver MNPs produced with increasing polymer concentration.

PVP controls the size of silver MNPs well with a standard deviation of 17%.[39] We show that PNIPAM achieves a similar

(58) Zhang, Z. T.; Zhao, B.; Hu, L. M. PVP protective mechanism of ultrafine silver powder synthesized by chemical reduction processes. *J. Solid State Chem.* **1996**, *121* (1), 105−110.

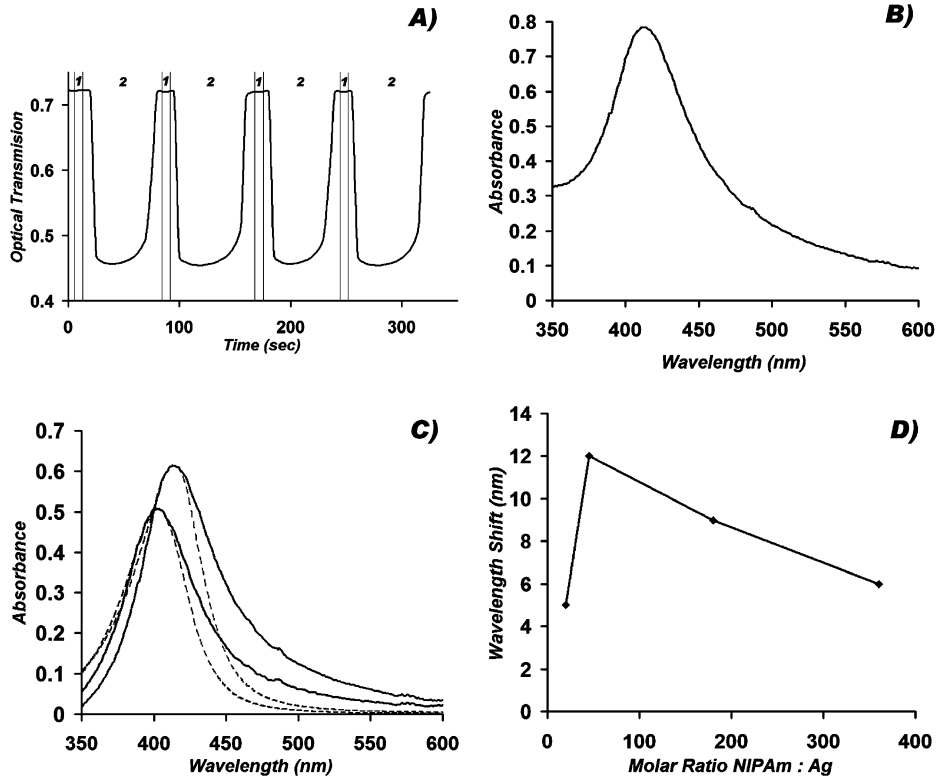

Figure 4. (A) Optical transmission of a colloidal suspension switched reversibly by increasing the temperature and allowing the sample to cool passively (PAR 180:1). (B) UV−vis spectra for a dilute sample of PAR 45:1 above the LCST. (C) UV−vis spectra (solid lines) after background subtraction below (dark) and above the LCST (light) for PAR 45:1 (solid lines) and the corresponding theoretical spectra (dashed lines). (D) Peak shift of the extinction spectra induced by the precipitation of the particles as a function of PAR.

control of the MNP size with a SD of 18−20%. PNIPAM also acts as a stabilizing agent, keeping the nanoparticles in solution for weeks. The lack of coalescence is also visible by the lack of a shoulder at larger wavelengths in the UV−vis extinction spectra, except for the case of low PAR (20:1) or for uncapped silver reduction. Experiments by Chen et al.[47] with short PNIPAM chains showed that the size could not be controlled as tightly, which may be caused by combining reduction and polymerization or by incomplete capping as has been suggested for other wet chemistry syntheses using a variety of stabilizing agents.[58−60] In contrast, the much larger PNIPAM polymers described here completely encapsulate the silver nanoparticles and influence their size in agreement with PVP results.[39]

The major advantages of using PNIPAM at room temperature to produce silver nanoparticles are the ability to work in aqueous solution, achieve a very fast but still well-controlled reduction using $NaBH_4$ as the agent, and have a one-step functionalization of a silver MNP with an environmentally sensitive polymer. The interaction between silver and PNIPAM appears to be strong enough to survive repeated precipitation and resolubilization cycles. The polymer protects the silver particles below and above the LCST from irreversible coalescence similar to surface-grafted PNIPAM−MNPs.[30,61] The polymer shell is 6−10 nm for high PARs in the dehydrated state but can be incomplete for low PARs.

The extinction spectra also suggest that the PNIPAM shell below the LCST induces a peak shift of about 2−17 nm, to 404 nm for low PARs and 419 nm for the higher PARs, as compared to the bare MNPs. PVP-coated silver nanoparticles show an extinction peak at 407 nm in water,[54] which is between the values measured for PNIPAM at low and high PARs. This can be explained by a higher incidence of incomplete capping at low PAR and by a higher incidence of more than one particle being encapsulated at high PAR, which explains the increased width, and the red shift in the maximum of the extinction peak as compared to the Mie model.[56] The stability of the colloidal suspension, the inability to precipitate PVP-coated MNPs in the presence of PNIPAM, and the ability to reversibly precipitate the PNIPAM−MNP colloid with a fast response suggest that PNIPAM and MNP are in close proximity and linked, even though the plasmon peak shift is very low for the lower PARs. In fact, precipitating the MNPs and heating the supernatant did not produce an LCST. Investigations into the interactions of the PNIPAM with the silver nanoparticles are under way.

Above the LCST, the spectral analysis indicates a dense polymer shell that induces a refractive index change of about 0.1 for all PARs. Although the shift in refractive index is of similar magnitude, the absolute values are lower at low PARs and higher for higher PARs than those for PNIPAM gels.[55] While this may be due to the lack of cross-links and a more loosely coiled polymer at low PARs, most likely it is due to the reasons that lead to the deviations from the Mie model already below the LCST as discussed before. This is supported by the constant FWHM below and above the LCST, which also shows that the electromagnetic interaction between metal particles is still weak above the LCST and that the particles must not touch as this would lead to a much larger shift to the red.[56]

(59) Yamamoto, M.; Kashiwagi, Y.; Nakamoto, M. Size-controlled synthesis of monodispersed silver nanoparticles capped by long-chain alkyl carboxylates from silver carboxylate and tertiary amine. *Langmuir* **2006**, *22* (20), 8581−8586.

(60) Pei, L. H.; Mori, K.; Adachi, M. Formation process of 2-D networked gold nanowires by citrate reduction of $AuCl_4$ and the shape stabilization. *Langmuir* **2004**, *20* (18), 7837−7843.

(61) Kim, D. J.; Kang, S. M.; Kong, B.; Kim, W. J.; Paik, H. J.; Choi, H.; Choi, I. S. Formation of thermoresponsive gold nanoparticle/PNIPAAm hybrids by surface-initiated, atom transfer radical polymerization in aqueous media. *Macromol. Chem. Phys.* **2005**, *206* (19), 1941−1946.

A three-stage process for the silver colloid production in the presence of a capping polymer has been suggested, consisting of a nucleation step, a growth step, and a step of agglomeration or stability of a specific size range of particles.[42] The crucial step in the production of monodisperse silver particles is that the nucleating stage and the growth stage overlap as little as possible. Despite the fast kinetics of the reduction process described here, the excellent size control suggests that the nucleation step is fast and enhanced by the stabilizing molecule PNIPAM. The short nucleation period may also promote a decrease in final particle size.

Variation of parameters such as PVP concentration, temperature, and order of addition of chemicals have led to non-spherical shapes due to the selective interaction of PVP with specific metallic crystal planes.[43] Similarly, block copolymers with two functional groups may allow for the creation of shapes with very high aspect ratios.[62] We are currently investigating both trends.

Conclusion

Using PNIPAM, with its LCST of 32 °C, as a nucleating and capping agent for the synthesis of silver nanoparticles, we have created nanoparticles with a PNIPAM shell in a two-step reaction. We have shown that the PNIPAM−Ag nanocomposites can be aggregated and resolubilized through many thermal cycles with a fast response and without hysteresis. The metal particles do not come into direct contact above the LCST but rather stay separated by the PNIPAM shell, and the plasmon resonance shifts by 5−12 nm. We have shown that our synthesis method produces Ag−PNIPAM nanoparticles, which are temperature sensitive due to PNIPAM's LCST. This switching behavior possibly also can be achieved optically by the local temperature increase due to light absorption at the surface plasmon wavelength.

Acknowledgment. The authors thank Dr. N. A. Peppas for helpful discussions and Dr. Ji-Ping Zhou for help with the electron diffraction. This work was supported in part by a grant from the Welch Foundation (F-1574) and by support from the Welch Foundation and SPRING through the Center for Nano and Molecular Science and Technology at the University of Texas at Austin. J.R.M. is a recipient of a fellowship from the Consejo Nacional de Ciencia y Tecnologia (CONACyT) and the ED Farmer Scholarship of the Mexican Center of the University of Texas at Austin.

LA7008336

(62) Iqbal, M.; Chung, Y.-I.; Tae, G. An enhanced synthesis of gold nanorods by the addition of pluronic (F-127) via a seed mediated growth process. *J. Mater. Chem.* **2007**, *17*, 335−342.